

Bogoliubov-Čerenkov radiation in a Bose-Einstein condensate flowing against an obstacle

I. Carusotto,¹ S.X. Hu,^{2,*} L. A. Collins,² and A. Smerzi^{2,1}

¹*CNR-BEC-INFM, Trento, I-38050 Povo, Italy*

²*Los Alamos National Laboratory, Los Alamos, 87544 NM*

We study the density modulation that appears in a Bose-Einstein condensate flowing with supersonic velocity against an obstacle. The experimental density profiles observed at JILA are reproduced by a numerical integration of the Gross-Pitaevskii equation and then interpreted in terms of Čerenkov emission of Bogoliubov excitations by the defect. The phonon and the single-particle regions of the Bogoliubov spectrum are respectively responsible for a conical wavefront and a fan-shaped series of precursors.

PACS numbers: 03.75.Kk, 41.60.Bq

The Čerenkov effect was first discovered in the electromagnetic radiation emitted by charged particles traveling through a dielectric medium at a speed larger than the medium's phase velocity [1]. A charge moving at the speed \mathbf{v} is in fact able to resonantly excite those modes of the electromagnetic field which satisfy the kinematic Čerenkov resonance condition $\omega_{em}(\mathbf{k}) = \mathbf{v} \cdot \mathbf{k}$: part of the kinetic energy of the particle is then emitted as Čerenkov radiation, with a peculiar frequency and angular spectrum [2]. Electromagnetic waves in a non-dispersive medium of refractive index n have a linear dispersion law relation $\omega_{em}(k) = ck/n$: the Čerenkov condition is then satisfied on a conical surface in k -space of aperture $\cos \phi = c/(nv)$, which corresponds to a conical wavefront of aperture $\theta = \pi/2 - \phi$ behind the particle. Thanks to the interplay of interference and propagation, much richer features appear in the spatial and k -space pattern of Čerenkov radiation in dispersive media [3, 4] and photonic crystals [5].

The concept of Čerenkov radiation can be generalized to any system where a source is uniformly moving through a homogeneous medium at a speed larger than the phase velocity of some elementary excitation to which the source couples. Many systems have been investigated in this perspective, ranging from e.m. waves emitted by the localized nonlinear polarization induced by a strong light pulse travelling in a nonlinear medium [6, 7], to the sonic waves generated by an airplane moving at supersonic velocities, to phonons in a polaritonic superfluid [8], and in a broader sense, to the surface waves emitted by a boat moving on the quiet surface of a lake [9]. In this Letter we compare our theoretical results of the density perturbation induced in a Bose-Einstein condensate (BEC) which flows against a localized obstacle at rest with the experimental images taken by the JILA group [10]. Modulo a Galilean transformation, the physics of a moving source in a stationary medium is in fact equivalent to the one of a uniformly moving medium interacting with a stationary defect. The experiment has been performed by letting a BEC expand at hypersonic speed against the lo-

calized optical potential of a far-detuned laser beam. The observed density profiles are successfully reproduced by numerically solving the time-dependent Gross-Pitaevskii equation and physically interpreted by a simple model of Čerenkov emission of Bogoliubov excitations by a weak defect.

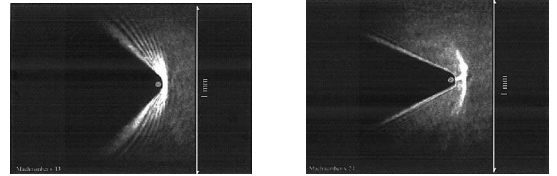


FIG. 1: Experimental [10] density profiles (integrated along z) of a BEC hitting an obstacle at supersonic velocities $v/c_s = 13$ (a) and 24 (b). The angles of the conical wavefronts are $\sin(\theta) = 0.73$ and $\sin(\theta) = 0.43$, respectively. The condensate flow is from the right to the left.

The experiment. The experimental results analyzed in this paper have been obtained by the JILA group [10] with a gas of $N = 3 \times 10^6$ Bose-Einstein condensed ^{87}Rb atoms confined in a cylindrically symmetric harmonic trap of frequencies $\{\omega_r, \omega_z\} = 2\pi\{8.3, 5.3\}$ Hz. The BEC is slightly cigar shaped, with the long axis pointing in the direction of gravity (z -axis), and a Thomas-Fermi radius in the $x - y$ plane of $31.6 \mu\text{m}$. At $t = 0$, the sign of the confining potential in the xy plane is inverted, so that the BEC undergoes an antitrapped expansion in the xy plane. At the same time, the confinement along z is switched off and replaced by a linear magnetic field gradient to cancel the effect of gravity. The obstacle consists of the repulsive potential of a blue-detuned dipole beam with a round Gaussian profile. The beam is directed in the z -direction and placed in the vicinity of the trapped condensate, and remains in this position during the experiment. Images of the BEC density profile after different expansion times t_{exp} are then taken by means of destructive absorption imaging. Two examples are shown in Fig.(1). The field of view is centered in the region

around the defect in order to observe the perturbation that it creates in the expanding condensate. In this region, the condensate is flowing from the right to the left. During the expansion, the condensate is strongly accelerated by the inverted harmonic trap, so that the local density at the defect position decreases in time, and the local speed v increases. As a result, images taken after increasing expansion times correspond to increasing values of the Mach number v/c_s , c_s being the local value of the sound velocity at the defect position. In Fig.1(a,b), the expansion times are $t = 33.6, 50$ ms, long enough for the flow to be strongly supersonic $v/c_s = 13, 24$. Downstream of the defect the atomic density is strongly reduced in a conical shadow region, separated from the unperturbed condensate region by a conical wavefront followed by a fan-shaped series of precursors which extends far in the upstream direction. For increasing Mach number v/c_s , the aperture of the shadow area decreases, as well as the spatial period of the precursors. Physical interpretations for all these features will be provided in the following.

Gross-Pitaevskii simulations. As a first step, the experimental data have been reproduced by a numerical simulation of the 3-dimensional, time-dependent Gross-Pitaevskii equation by means of a real-space-product finite element discrete-variable-representation [11], a numerical method that has already seen effective service in solving several large-scale computational problems involving BECs [12]. Results for the exact parameters of the experiment are shown in Fig.2(a,b).

The laser obstacle consists of a repulsive potential with a Gaussian shape $V(r) = V_{max} \exp(-2r^2/w^2)$. The maximum height $V_{max} = 4961 \hbar\omega_r$ of the potential is much larger than the chemical potential of the BEC in the initial trapped configuration and its width $w = 17 \mu\text{m}$ is ~ 50 times larger than the BEC healing length: the obstacle can therefore be considered, for all practical purposes, as a rigid cylinder. In Figs.2(a,b), the defect is situated at a distance of respectively $d = 75, 87 \mu\text{m}$ from the condensate center and the imaging times are $t = 33.6, 50$ ms. The density profiles emerging from the simulations are in agreement with the experimental findings of Fig.(1). The Mach numbers in the GPE simulations are 12.4 (a) and 23.8 (b), and the angles of the conical wavefronts delimiting the shadow areas are $\sin(\theta) = 0.7$ (a) and $\sin(\theta) = 0.48$ (b). The values of the angles are in excellent agreement with the experimental ones: $\sin(\theta) = 0.73$ and $\sin(\theta) = 0.43$ for a Mach number 13 and 24, see Fig.(1). The GPE simulations also reproduce the fan of precursors moving upstream of the defect [13]. By comparing panels (a) and (b) of Fig.2, one sees that the longer the imaging time, the longer the spatial distance the precursors have traveled.

Both the spatial period of the precursors, and the aperture of the cone decrease for an increasing Mach number v/c_s , but this latter is always significantly larger than the Mach angle such that $\sin(\theta) = v/c_s$. As the flow ve-

locity of the expanding BEC is not uniform, but rather radial, the geometric angle formed by the tangent of the obstacle through the BEC center and the line joining the obstacle and the BEC centers has to be added to the Mach angle. In addition to this, the geometrical shadow effect provides a simple, ballistic, explanation also for the strong density reduction inside the cone. This interpretation has been verified by repeating the simulations for obstacles of smaller size: as it is shown in Fig.2(cd), the aperture of the cone significantly decreases and asymptotically approaches the Mach angle in the limit of small defect, see Fig.(3).

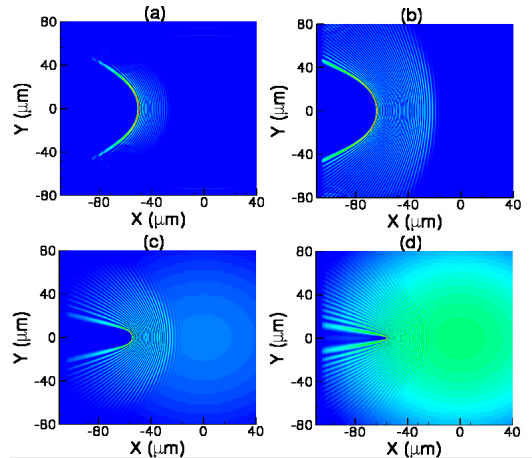


FIG. 2: GPE density profiles integrated along the z -direction obtained with different expansion times and sizes of the obstacle : a) $t = 33.6$ ms, $w=17 \mu\text{m}$.; b) $t = 50$ ms, $w=17 \mu\text{m}$.; c) $t = 38.4$ ms, $w=3.74 \mu\text{m}$.; d) $t = 38.4$ ms, $w=0.374 \mu\text{m}$.

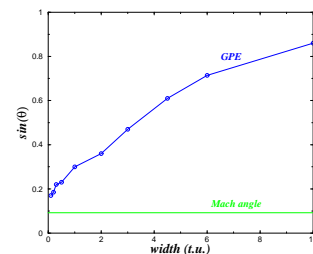


FIG. 3: Conical wave front aperture as a function of the obstacle width (in “trap units”, 1 t.u. = $3.74 \mu\text{m}$) calculated with GPE. The green line is the Mach angle.

Bogoliubov-Čerenkov theory. A simple way of getting a qualitative physical understanding of the experimental and numerical results is to use an approximate theory where the condensate is assumed to be homogeneous and uniformly flowing at a constant speed \mathbf{v}_0 and the defect, localized around $\mathbf{x} = 0$, induces a weak density perturbation [8, 15, 16]. Under this approximations, analytical results for the stationary solution of the GPE can

be obtained by means of the Bogoliubov linear response theory. As boundary condition, an incident plane wave of the form $\psi_0(\mathbf{x}, t) = \psi_0 e^{i(\mathbf{k}_0 \mathbf{x} - \omega_0 t)}$ is taken, where we have set $\hbar \mathbf{k}_0 = m \mathbf{v}_0$, $\rho_0 = |\psi_0|^2$, $\hbar \omega_0 = m \mathbf{v}_0^2/2 + g \rho_0$. Here $g = 4\pi \hbar^2 a_s/m$ in terms of the atomic s -wave scattering length a_s and mass m . The sound velocity is $c_s = \sqrt{g \rho_0/m}$.

The BEC wavefunction $\psi(\mathbf{x}, t) = [\psi_0(\mathbf{x}) + \delta\psi(\mathbf{x}, t)] e^{-i\omega_0 t}$ is the sum of the unperturbed wavefunction $\psi_0(\mathbf{x}, t)$ plus the small perturbation $\delta\psi(\mathbf{x}, t)$. Introducing the compact notation $\delta\vec{\psi}(\mathbf{x}, t) = (\delta\psi(\mathbf{x}, t), \delta\psi^*(\mathbf{x}, t))^T$, the evolution can be written in the form of a linear equation [8]:

$$i\hbar \frac{\partial}{\partial t} \delta\vec{\psi} = \mathcal{L} \cdot \delta\vec{\psi} + \vec{F}_d, \quad (1)$$

with a source \vec{F}_d proportional to the defect potential V_d :

$$\vec{F}_d(\mathbf{x}) = V_d(\mathbf{x}) \begin{pmatrix} \psi_0(\mathbf{x}) \\ -\psi_0^*(\mathbf{x}) \end{pmatrix}. \quad (2)$$

The Bogoliubov matrix \mathcal{L} has the usual form:

$$\mathcal{L} = \begin{pmatrix} -\frac{\hbar^2}{2m} \nabla^2 + \rho_0 g & \rho_0 g e^{2i\mathbf{k}_0 \mathbf{x}} \\ -\rho_0 g e^{-2i\mathbf{k}_0 \mathbf{x}} & -\left[-\frac{\hbar^2}{2m} \nabla^2 + \rho_0 g \right] \end{pmatrix}. \quad (3)$$

and its eigenvalues give the energies of the elementary excitations of the system around the unperturbed stationary state. In our specific case of a homogeneous and homogeneously flowing BEC, the Bogoliubov dispersion law is

$$\omega(\mathbf{k}) = \mathbf{v} \cdot (\mathbf{k} - \mathbf{k}_0) \pm \sqrt{\frac{\hbar(\mathbf{k} - \mathbf{k}_0)^2}{2m} \left(\frac{\hbar(\mathbf{k} - \mathbf{k}_0)^2}{2m} + 2g\rho_0 \right)} \quad (4)$$

As we can see in the dispersion spectra shown in the left column of Fig.4, the main effect of the flow consists of the additional term $\mathbf{v}_0 \cdot (\mathbf{k} - \mathbf{k}_0)$ which tilts the dispersion and add \mathbf{v}_0 to the propagation group velocity of all the Bogoliubov excitations. The \pm branches correspond to respectively the particle- and the hole-like branches of the Bogoliubov dispersion, and are images of each other under the transformation $\mathbf{k} \rightarrow 2\mathbf{k}_0 - \mathbf{k}$, $\omega \rightarrow -\omega$. The steady state in the presence of the defect potential V_d is obtained from the motion equation (1) as:

$$\delta\vec{\psi}_d = -(\mathcal{L} - i0^+ \mathbf{1})^{-1} \cdot \vec{F}_d. \quad (5)$$

The infinitesimal imaginary term is required to satisfy the boundary condition that at $t = -\infty$ no Bogoliubov excitations were present. As can be easily seen from the resonant denominator, the time-independent defect potential excites the Bogoliubov modes whose energy is $\omega(\mathbf{k}) = 0$. Graphically, these \mathbf{k} modes can be identified in the plots in the left column of Fig.4 as the intersection points of the dispersion surface $\omega(\mathbf{k})$ with the $\omega = 0$ plane. Modulo a Galilean transformation, this condition corresponds

to the usual Čerenkov resonance condition [2]. Depending on whether the flow speed is slower or faster than the speed of sound in the BEC, two regimes can be identified.

In the subsonic regime $v_0 < c_s$, no intersection exists at $\mathbf{k} \neq \mathbf{k}_0$, which physically means that no Bogoliubov mode can be resonantly excited by the defect. The BEC is superfluid and can flow around the defect without suffering any dissipation, in agreement with the Landau criterion of superfluidity.

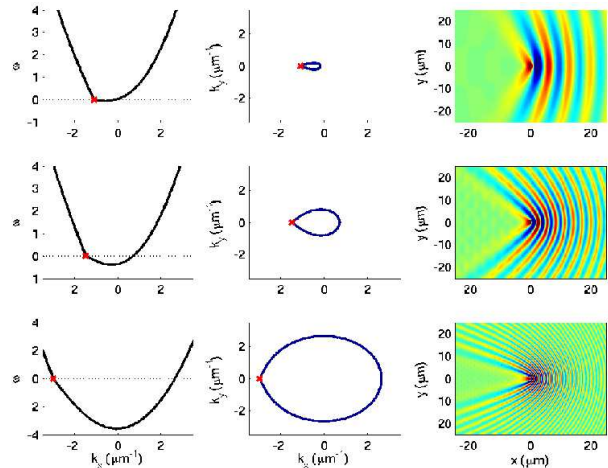


FIG. 4: Dispersion of Bogoliubov modes (left column), curve Γ in \mathbf{k} space describing the resonantly excited Bogoliubov modes (center column) and spatial density profile (right column). The supersonic flows are $v_0/c_s = 1.1, 1.5, 3$ in each row, respectively.

On the other hand, in the supersonic regime, $v_0 > c_s$, the set of \mathbf{k} vectors satisfying $\omega(\mathbf{k}) = 0$ is not empty, but rather corresponds to the closed curve Γ shown in the central column of Fig.4. Some of the kinetic energy associated to the flow is therefore dissipated as radiation of Bogoliubov modes. In real space, the perturbation radially propagates from the defect with a velocity fixed by the group velocity of the mode $\mathbf{v}_g = \nabla_{\mathbf{k}} \omega$. For each mode \mathbf{k} , the direction of \mathbf{v}_g corresponds to the outward normal to the curve Γ . Since we are here considering a stationary state, the density perturbation propagates to infinity in all available directions. Yet, even though Γ is a closed curve, the possible directions of the group velocity do not fill the whole unit sphere: because of the singularity at \mathbf{k}_0 there exists a region of excluded directions, which in the plots in the left column of Fig.4 correspond to the unperturbed region inside the Čerenkov cone.

The spatial profiles of the density perturbation predicted by the linear theory can be understood by analyzing the different regions of Γ . Close to the singular point at $\mathbf{k} = \mathbf{k}_0$, the curve consists of two straight lines separated by an angle 2ϕ defined by the usual Čerenkov condition $\cos \phi = c_s/v_0$. This region corresponds to the small wavevector part of the Bogoliubov

spectrum, which is indeed linear and allows for an interpretation of the corresponding radiation in terms of the usual Čerenkov effect in non-dispersive media. In the plots in the right column of fig.4, the strongest density perturbation lies on the Mach cone of aperture θ such that $\sin \theta = c_s/v_0$, and directed in the downstream direction; being the flow velocity larger than the sound velocity, the density perturbation is dragged away from the defect. The rounded region of Γ for \mathbf{k} nearly anti-parallel to \mathbf{k}_0 is absent in the standard theory of the Čerenkov effect in non-dispersive media, and originates from the quadratic, single-particle-like, part of the Bogoliubov spectrum. The group velocity at the right-most point of Γ is equal to $v_g = [c_s^2/v_0 - v_0]$ so that the perturbation propagates in the upstream direction with respect to the BEC flow and gives an oscillating density modulation of wave-vector $|\mathbf{k} - \mathbf{k}_0| = 2m(v_0^2 - c_s^2)^{1/2}/\hbar$. This is a direct consequence of matter-wave interference between the incident BEC and the scattered wave off the obstacle [17]. In the intermediate points on the curve, there is a one-to-one correspondence between excited Bogoliubov modes of wavevector \mathbf{k} and the direction $\hat{\mathbf{x}}$ such that $\hat{\mathbf{x}}$ is parallel to the group velocity $\mathbf{v}_g(\mathbf{k})$. For each point $\mathbf{x} = x\hat{\mathbf{x}}$ in space, this correspondence determines the wavevector \mathbf{k} of the Bogoliubov mode that is able to reach it, and consequently the wavevector $\mathbf{k}_m = \mathbf{k}_0 - \mathbf{k}$ of the density modulation in its vicinity. Despite the underlying approximations, the features of the Bogoliubov theory qualitatively reproduce the full GPE simulations and therefore clarify the interpretation in terms of Čerenkov waves of the experimental findings.

In conclusion, we have presented a combined theoretical and experimental study of the response of a Bose-Einstein condensate flowing against a localized obstacle at supersonic velocity [18]. A numerical study of the full Gross-Pitaevskii equation has been performed to fully simulate the experiment. The findings are in agreement with the experiment, and have been interpreted within the Bogoliubov approximation in terms of the Čerenkov emission of phonons by the defect: this creates a Mach cone density modulation downstream of the defect, as well as an additional upstream fan-shape perturbation, which originates from the interference between the particle-like Bogoliubov excitations and the underlying BEC. For growing strengths and sizes of the obstacle, the numerical study shows a continuous evolution of the density modulation towards a soliton train [19], as typical of the dynamical evolution of shock-waves in dispersive, dissipationless nonlinear 1D wave equations [20].

Acknowledgments. We are indebted with E.A. Cornell and P. Engels for providing us the experimental data shown in Fig.(1). AS gratefully thanks P. Engels for several clarifications on the experimental results and P. Krapivsky for discussions on the formation of shock

waves in nonlinear systems. IC is grateful to C. Ciuti for continuous discussions on the Čerenkov effect in quantum fluids. We also acknowledge a collaboration with C. Menotti at an early stage of the work. Work partially supported by the U.S. Department of Energy, contract DE-AC52-06NA-25396.

* Present address: Laboratory for Laser Energetics, University of Rochester, 250 E. River Road, Rochester, NY 14623

- [1] L.D. Landau and E.M. Lifshitz, *Electrodynamics of continuous media* (Pergamon Press, Oxford, 1987).
- [2] J. V. Jelley, *Čerenkov radiation and its applications*, Pergamon Press, 1958.
- [3] G. N. Afanasiev, V. G. Kartavenko, and E. N. Magar, *Physica B* **269**, 95 (1999).
- [4] I. Carusotto, *et al.*, *Phys. Rev. Lett* **87**, 064801 (2001).
- [5] C. Luo *et al.*, *Science* **299**, 368 (2003).
- [6] D. H. Auston *et al.*, *Phys. Rev. Lett.* **53**, 1555 (1984)
- [7] T. E. Stevens *et al.*, *Science* **291**, 627 (2001)
- [8] I. Carusotto, C. Ciuti, *Phys.Rev.Lett.* **93**, 166401 (2004).
- [9] G.B. Whitham, *Linear and Nonlinear Waves*, Wiley-Interscience, New-York, 1974.
- [10] E. A. Cornell and P. Engels (private communication); see also E. Cornell's talk at the *KITP Conference on Quantum Gases* (U. California, Santa Barbara, 2004) at http://online.itp.ucsb.edu/online/gases_c04/cornell/.
- [11] B. I. Schneider *et al.*, *Phys. Rev.* **E 73**, 036708 (2006).
- [12] J. Denschlag *et. al.* *Science* **287**, 97 (2000); B. Anderson *et. al.* *Phys. Rev. Lett.* **86**), 2926 (2001).
- [13] Differently from [14], no evidence for the shedding of vortices was found in our simulations.
- [14] B. Jackson, J.F. McCann and C.S. Adams, *Phys. Rev. Lett.* **80** 3903 (1998); T. Winiiecki, J.F. McCann and C.S. Adams, *Phys. Rev. Lett.* **26** 5186 (1999).
- [15] G.E. Astrakharchik and L.P. Pitaevskii, *Phys. Rev.* **A70**, 013608 (2004).
- [16] S. Ianeselli *et al.*, *J.Phys.B* **39**, S135 (2006).
- [17] In the case of a very fast flow or non interacting atoms, $v_0/c_s = \infty$, the Bogoliubov dispersion reduces to the free particle one $\omega(\mathbf{k}) = \hbar\mathbf{k}^2/2m$ and the locus of excited Bogoliubov modes is a ring of radius $|\mathbf{k}_0|$. For a weak defect of strength C , the stationary state is $\psi(\mathbf{x}, t) = \left[e^{i\mathbf{k}_0\mathbf{x}} + \frac{C}{|\mathbf{x}|} e^{i\mathbf{k}_0|\mathbf{x}|} \right] e^{-i\omega_0 t}$ and the density perturbation consists of a series of fan-shaped parabolic wavefronts $r^2 = N^2\lambda_0^2 - 2N\lambda_0 z$ (the integer $N \geq 0$, $\mathbf{v}_0 = v_0\hat{z}$ and $\lambda_0 = 2\pi/k_0$) due to interference of the incident and the scattered matter waves. More details in C. Ciuti and I. Carusotto, *Phys. Stat. Sol.* (b) **242**, 2224 (2005).
- [18] During proof-reading, a related preprint has appeared: Yu. G. Gladish, G. A. El, A. Gammal, and A. M. Kamchatnov, cond-mat/0611149.
- [19] G. A. El, A. Gammal, and A. M. Kamchatnov, *Phys. Rev. Lett.* **97**, 180405 (2006).
- [20] P. Leboeuf and N. Pavloff, *Phys. Rev.* **A 64**, 033602 (2001); C. Menotti *et al.*, *Phys. Rev.* **A 70**, 023609 (2004)